Hindawi Publishing Corporation
Advances in Meteorology
Volume 2015, Article ID 247531, 12 pages
http://dx.doi.org/10.1155/2015/247531

Research Article

Study of Aerosols' Characteristics and Dynamics over the Kingdom of Saudi Arabia Using a Multisensor Approach Combined with Ground Observations

Ashraf Farahat,[1,2] Hesham El-Askary,[3,4,5] and Abdulaziz Al-Shaibani[6]

[1]*Department of Prep Year Physics, College of Applied and Supporting Studies, King Fahd University of Petroleum and Minerals, Dhahran 31261, Saudi Arabia*
[2]*Department of Physics, Faculty of Science, Alexandria University, Moharam Beek, Alexandria 21522, Egypt*
[3]*Schmid College of Science and Technology, Chapman University, Orange, CA 92866, USA*
[4]*Center of Excellence in Earth Systems Modeling and Observations, Chapman University, Orange, CA 92866, USA*
[5]*Department of Environmental Science, Faculty of Science, Moharam Beek, Alexandria University, Alexandria 21522, Egypt*
[6]*Department of Earth Science, King Fahd University of Petroleum and Minerals, Dhahran 31261, Saudi Arabia*

Correspondence should be addressed to Hesham El-Askary; elaskary@chapman.edu

Received 25 August 2014; Revised 28 November 2014; Accepted 9 December 2014

Academic Editor: Slobodan Nickovic

This study covers various aspects of the aerosol distribution and characteristics, namely, optical depth climatology, absorption characteristics, and their microphysical properties over four regions in Saudi Arabia using satellite and ground observations including MODIS/Terra and Aqua, OMI, MISR/Terra, AERONET, and CALIPSO for the period April 2003–January 2013. The study includes cities in the North Western, Western, Eastern provinces of Saudi Arabia and in the Rub al Khali desert or Empty Quarter. Satellite and ground observations showed that the dust season extends from April to August with prominent peaks yet with high anthropogenic contribution late summer and early fall. Analysis shows an increase in the aerosol concentration during March 2009 which could be attributed to a major dust storm during that time. Comparing the AOD time series over regions 1–3 and region 4 (desert) we observe monthly and annual variability with no recurrence pattern over the years. The Aqua Deep Blue AOD_{550} data shows a single peak pattern that occurs over region 4 during the spring season known for its frequent dust events. OMI data shed the light on the presence of higher air pollution levels over region 3, representing the oil rich eastern province of Saudi Arabia.

1. Introduction

Aerosols' impact on the regional climate and their ultimate connections to the Earth's global climate system and hence forcing has been observed through their optical and microphysical properties [1–5]. Thus, improving our understanding of aerosol properties and characterization is imperative especially over mega and highly populated cities where aerosols have major impacts on human health [6–9]. The kingdom of Saudi Arabia is one of the major sources of aerosols in the world, including natural and anthropogenic components [10, 11]. Yet, it still lacks for better characterization of its atmospheric aerosols properties with significant shortage of in situ observations. Over the Middle East, dust sources extend from the north of the Tigris-Euphrates basin to the coast of Oman, yet dust activity is quite complex and widely impacted by seasonal variability [12]. Temporal and spatial characteristics of Saudi Arabian dust storms, with focus on associated air parcel trajectories, have been investigated using dust concentrations and geochemistry of aerosols, station, and gridded weather observations and remotely sensed aerosol observations [13–15].

Using PM_{10} concentrations, recorded by the King Abdel Aziz City for Science & Technology (KACST) monitoring network during 2000–2003, nine local and four external dust sources have been identified, in association with seven

types of dust storms, triggered by seasonal distribution of meteorological conditions, yet dominated by Haboob (~42%) and Shamal (~37%). A thorough investigation of one of the most intense dust storms experienced in Saudi Arabia over the last two decades that struck Riyadh and lasted several hours on March 10th, 2009 was conducted [16]. Significant changes of aerosol and meteorological parameters were observed with air pressure rapidly increasing by 4 hPa, temperature decreasing by 6°C, relative humidly increasing from 10% to 30%, Aerosol Optical Depth (AOD) at 550 nm increasing from 0.396 to 1.71, and Angstrom Exponent (AE) rapidly decreasing from 0.192 to −0.078. On the other hand, seasonality and aerosols' concentration variability impacting cloud properties and serving as condensation nuclei were studied over the Arabian Sea using satellite and ground observations [17, 18], and over other surrounding locations in Northern Africa and Gulf region [19–29]. According to [18] seasonal variations are clearly found in the shape and magnitude of the volume size distribution of the coarse size mode due to dust emission.

A model for PM_{10} dust emission was constructed by [30], using the concept of a threshold friction velocity which is dependent on surface roughness that in turn was correlated with geomorphology or soil properties. This was applied for Kuwait, Iraq, Syria, Saudi Arabia, the United Arab Emirates, and Oman. The model results agreed quantitatively with measurements at four locations in Saudi Arabia and one in Kuwait for one major dust event (>1000 $\mu g/m^3$). On the other hand [31] incorporated a two-stream scattering scheme based on the delta-Eddington approximation into the Florida State University Limited Area Model for computing the shortwave radiative fluxes due to dust aerosols over the Saudi Arabian region and to study their impact on synoptic-scale systems and the diurnal cycle over the region. The average diameter of dust particles collected during a dust storm at various heights near Riyadh was tested by [32]. It was found that most of the particle size distributions can be described by a lognormal or normal distribution depending on the storm condition and height. The average diameter of sand/dust particles decreases with the increase of height according to a power law.

In this paper, we present a detailed climatological analysis of the optical and microphysical aerosol properties using satellite observations over four main selected regions in Saudi Arabia; criteria of selection follow, highlighted in Figure 1. Furthermore, we discuss patterns of aerosol transport and characteristics during the significant March 10, 2009 dust storm as well as aerosol optical and physical characteristics as an extension of the work performed by [16]. Data from two AErosol RObotic NETwork (AERONET) ground based stations, namely, the Solar Village (long: 46.397 lat. 24.907) and MASDAR (long. 54.617 lat. 24.442) (indicated by 5 and 6, resp., in Figure 1), are also used for validation purposes. The two stations are yet not included in our four selected regions of interest but are seen of great importance for comparison between deserts and urban areas. Aerosols in general have regional behavior and long-range transport may be a factor; therefore, using the ground data is seen as a needed addition.

Region 1 represents the North Western (NW) cities of Saudi Arabia, where temperature ranges from ~46°C during summer to ~−6°C during winter, with rain fall during the winter months from November to March. The NW region has small population of less than 600,000 and contains the Tabuk industrial city on an area of 1.4 million square meter and known for its petrochemical, plastic, aluminum, and steel industries. Region 2 represents the Western Province (WP) of Saudi Arabia that includes three major cities, namely, Jeddah, Mecca, and Madinah known for their high population especially during Muslims' pilgrimage season (Hajj), which is said to be the largest people gathering in the world with more than 2 million visits per year. Particulate pollution is a serious problem in the city of Mecca and in the neighboring regions due to particles emitted by traffic during the Hajj season [33, 34]. Moreover, the city of Mecca is located in a valley in approximately the middle of the Sarawat mountain range that produces large concentrations of airborne sand and anthropogenic aerosols. The WP retains its very warm temperature in winter ~18°C increasing to ~40°C during summer, with sparse rain falls between November and January. Region 3 represents the East province (EP) of Saudi Arabia, containing one of the largest industrial complexes in the Middle East including steel mill, oil refinery, world's largest desalination plants, electric power, and petrochemical products such as plastic and fertilizers. The climate of the EP is tropically hot and relatively humid with temperature ranging from ~46°C during the summer to ~13°C during the winter [35]. Finally, region 4 is located at the southern Saudi Arabia and represents the Rub al Khali Desert or Empty Quarter (EQ). The EQ is a massive source of aerosols as it covers an area of ~560,000 km^2 with daily maximum temperature reaching as high as 56°C and receiving annual rainfall of less than 30 mm.

Figure 1: Map of Saudi Arabia including the four regions considered in this study represented by the cities of Tabuk, Mecca, and Dhahran and Rub al Khali (Empty Quarter) Desert. AERONET Solar Village and MASDAR locations are indicated by 5 and 6.

2. Data Sets and Methods

In this work we utilized aerosol measurements from a number of sensors to leverage the wide variety of aerosol

parameters available from these sensors, which include the Moderate Resolution Imaging Spectroradiometer (MODIS) aboard the Terra and Aqua satellites and the Ozone Monitoring Instrument (OMI) on the Aura satellite to investigate the aerosol optical properties; the Multi-angle Imaging SpectroRadiometer (MISR) instrument on Terra to examine microphysical properties of the aerosols including size and shape; Cloud-Aerosol Lidar and Infrared Pathfinder (CALIOP) sensor on CALIPSO satellite to identify different aerosol types and vertical distribution. Ground-based measurements used in this analysis include the multiyear aerosol AERONET measurements [36] at two sites mentioned above. The HYSPLIT (Hybrid Single-Particle Lagrangian Integrated Trajectory) model version 4 was used to generate air mass forward trajectories. The HYSPLIT model is the latest version of an integrated system for computing air parcel trajectories, dispersion, and deposition simulations [37]. The above-mentioned data will be used to characterize the apparent complex dynamics of the aerosols over the Kingdom that are dominated by coarse mode dust aerosols from the desert, modified and mixed with fine anthropogenic aerosol.

2.1. MODIS/Terra and MODIS/Aqua. MODIS/Terra and MODIS/Aqua instruments provide a number of validated aerosol products that include AOD at 10 km resolution over water and over land [38, 39]. The AOD uncertainty is ±0.05 (±0.15∗AOD) over land and ±0.03 (±0.05∗AOD) over ocean. Uncertainty in the monthly average fine fraction aerosol optical depth is ±20% [38]. Over the desert region we use the Deep Blue product rather than the standard AOD product because the latter is retrieved using the dark-target approach [40] at near-infrared wavelengths (2.1 and 3.8 μm) [41]. The two blue channels (0.412 and 0.470 mm) allow the Deep Blue algorithm to be more sensitive to aerosols over bright surfaces for which surface reflectance is relatively small to infer aerosol properties [42]. The MODIS Deep Blue algorithm primarily uses the UV channels to provide aerosol retrievals over deserts and other areas where the operational cannot. The uncertainties of the Deep Blue product are reported to be around 25–30% [43]. The recent release of a new 3-km resolution aerosol product in the MODIS Collection 6 dataset [44] is highly advantageous for studying small regions such as those highlighted in the present study.

2.2. MISR/Terra. MISR/Terra operational aerosol retrievals performed at 17.6 km horizontal resolution include some information about particle size, shape, and single-scattering albedo, in addition to AOD which will be used in this study [45–48]. A global comparison of coincident MISR and AERONET sunphotometer data showed that overall, about 70% to 75% of MISR AOD retrievals fall within 0.05 or 20%∗AOD, and about 50% to 55% are within 0.03 or 10%∗AOD, except at sites where dust or mixed dust and smoke are commonly found [48, 49]. Here, we have analyzed the Level 3 monthly aerosol product averaging select Level 1 and Level 2 parameters over daily, monthly, seasonal, and annual time periods from January 2003 to August 2009 to study aerosols shape and size.

2.3. CALIPSO. CALIPSO is a Franco-American mission that supplies a unique dataset of atmospheric vertical profiles measured by CALIOP on-board the satellite with a 30-m vertical resolution. CALIPSO data releases began in mid-June 2006 and include Level 1 radiances, a Level 2 vertical feature mask, and cloud and aerosol layer products [50].

2.4. OMI/Aura. OMI/Aura provides the (UltraViolet Aerosol Index) UVAI data [51–53]. The UVAI is a product of the standard OMI aerosol retrieval, which indicates the UV absorbing aerosols [53]. Absorbing aerosols such as carbonaceous aerosols, desert dust, and volcanic ash above the boundary layer yield positive UVAI values (>1), whereas nonabsorbing small particle aerosols yield small negative values [53]. Absorbing aerosols in the boundary layer may produce small UVAI values (<0.5) that make it difficult to separate their signal from the background noise. Given the large size (13 × 24 km at nadir) of the OMI pixels, subpixel cloud contamination is a persistent problem resulting in the overestimation of AOD and underestimation of the single-scattering coalbedo [53].

2.5. AERONET. AERONET federation of Cimel sunphotometers provide daytime AOD measurements every 15-min on average covering the 340–1600 nm wavelength range with typical AOD uncertainties of ±0.015 [36, 54, 55]. AERONET AODs are derived from direct-beam solar measurements, and some information about particle size and indices of refraction are derived from sky-scans which will be used in this study from the stations mentioned in Section 1.

3. Results and Discussion

3.1. Analysis of Aerosol Optical Depth (AOD). In this study, the MODIS Terra and Aqua AOD data were acquired to investigate the aerosols load, characteristics, extent, and temporal variability over three Saudi Arabian subregions including Tabuk (34.70°E to 36.21°E and 27.60°N to 28.99°N); Mecca (38.42°E to 40.82°E and 20.50°N to 22.28°N), and Dhahran (49.98°E to 50.19°E and 26.21°N to 26.56°N) (Figure 1). These regions are selected to represent the NW, W, and E areas of Saudi Arabia, respectively, for spatial representation of aerosols behavior. Figures 2(a), 2(b), and 2(c) show the AOD monthly mean at 550 nm over Tabuk, Mecca, and Dhahran from April 2003 till January 2013. Figure 2(d) shows the monthly Deep Blue at 550 nm over Rub al Khali (Empty Quarter) Desert (52°E to 52.4°E and 19.6°N to 20°N) during the same period. Due to the relatively small reflectance over the Rub al Khali Desert, we used the Deep Blue algorithm for its larger sensitivity to aerosols over bright surfaces as discussed in Section 2.1. Comparing the AOD monthly data over the four regions shows monthly and annual variability with no recurrence pattern over the years. A sudden increase in the aerosol concentration is observed during 2009 over region 3 (EP) that can be attributed to the major March 2009 dust event in Saudi Arabia as well as to some industrial activities in that region [14]. This significant observed increase in the AOD concentration average values over Dhahran (Figure 2(c)) during 2008-2009 yet has

Table 1: Annual AOD means for Terra and Aqua over regions 1–3 and for Aqua Deep Blue over region 4 (desert).

Year	Annual mean of Terra AOD Regions			Annual mean of Aqua AOD Regions			Aqua Deep Blue AOD Regions
	1	2	3	1	2	3	4
2003	0.24 ± 0.02	0.47 ± 0.05	0.56 ± 0.11	0.21 ± 0.02	0.42 ± 0.04	0.47 ± 0.07	0.29 ± 0.04
2004	0.23 ± 0.02	0.35 ± 0.02	0.40 ± 0.04	0.20 ± 0.02	0.33 ± 0.02	0.38 ± 0.03	0.20 ± 0.02
2005	0.24 ± 0.02	0.40 ± 0.07	0.43 ± 0.04	0.22 ± 0.01	0.35 ± 0.03	0.37 ± 0.03	0.24 ± 0.03
2006	0.24 ± 0.01	0.36 ± 0.03	0.41 ± 0.03	0.22 ± 0.02	0.35 ± 0.03	0.40 ± 0.03	0.28 ± 0.04
2007	0.26 ± 0.03	0.38 ± 0.03	0.51 ± 0.06	0.20 ± 0.02	0.38 ± 0.02	0.44 ± 0.04	0.27 ± 0.03
2008	0.25 ± 0.02	0.41 ± 0.04	0.66 ± 0.10	0.20 ± 0.02	0.44 ± 0.05	0.63 ± 0.11	0.32 ± 0.06
2009	0.24 ± 0.02	0.38 ± 0.03	0.65 ± 0.10	0.19 ± 0.01	0.38 ± 0.03	0.71 ± 0.12	0.26 ± 0.04
2010	0.29 ± 0.02	0.39 ± 0.05	0.48 ± 0.05	0.27 ± 0.02	0.42 ± 0.06	0.48 ± 0.05	0.24 ± 0.03
2011	0.22 ± 0.01	0.40 ± 0.04	0.53 ± 0.07	0.20 ± 0.02	0.44 ± 0.06	0.50 ± 0.07	0.31 ± 0.05
2012	0.27 ± 0.04	0.40 ± 0.04	0.52 ± 0.07	0.24 ± 0.03	0.44 ± 0.05	0.50 ± 0.06	0.33 ± 0.05

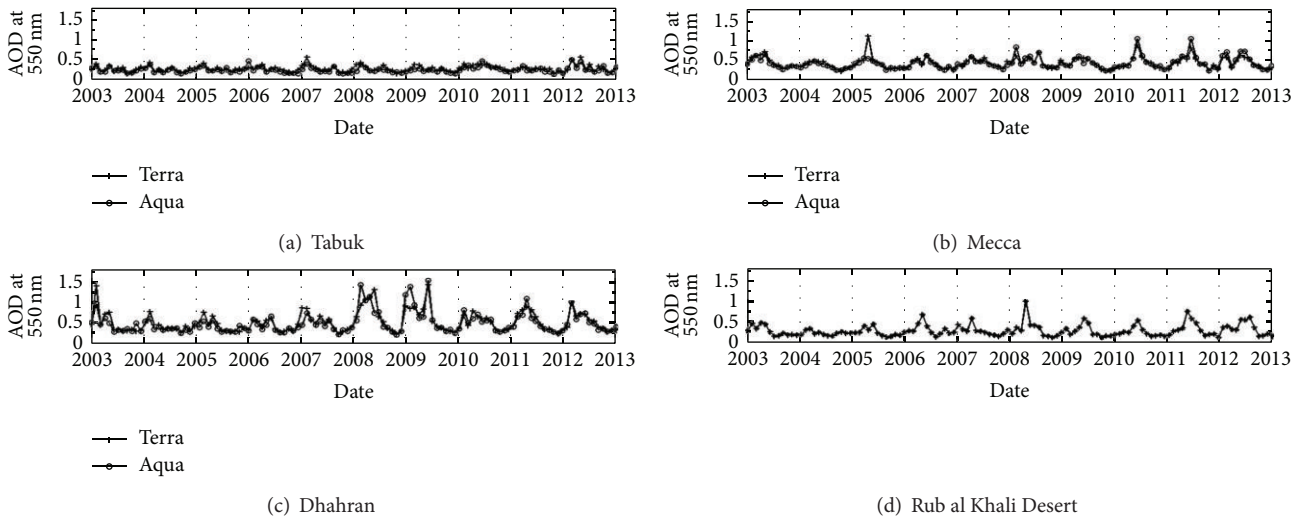

Figure 2: Time series plot of MODIS AOD at 550 nm using Terra and Aqua over (a) Tabuk, (b) Mecca, and (c) Dhahran and Aqua Deep Blue data over (d) Rub al Khali (Empty Quarter) Desert.

a slight impact on Mecca (Figure 2(b)) as compared to Rub Al Khali (Figure 2(d)) implying the local nature of this event. On the other hand, the Aqua Deep Blue AOD_{550} data over Rub al Khali Desert (Region 4) (Figure 2(d)) shows a single peak pattern annually taking place during the spring season during which dust events are dominant. Table 1 shows the average AOD with the standard errors over regions 1–4. To examine the AOD background level over the Kingdom, monthly means climatology over regions 3 and 4 using MODIS standard AOD and Deep Blue, respectively, at 550 nm is calculated and represented (Figures 3(a) and 3(b)) with standard vertical error bars of the monthly mean values. The monthly MODIS climatological means shows a cycle with minimum AOD during autumn and winter months and then peaks during spring and summer months. The maximum annual mean AOD_{550} from Aqua and Terra is ~0.82 ± 0.06, ~0.72 ± 0.05, respectively, while the minimum annual mean is ~0.28 ± 0.06, ~0.28 ± 0.05, respectively. It is clear that there is still a relatively high AOD background observed over the selected regions which can be associated with the industrial pollution and petrochemical industry active in region, which is typical of industrial cities in developing countries [7, 56, 57].

Such high background AOD levels would have an indirect impact on the local climate and precipitation levels. Hence, the relation between the mean precipitation rate and AOD levels is investigated and as a result, monthly climatology of the mean precipitation rate over region 3 is additionally plotted to (Figure 3(a)) during the period 2003–2013. Minimum precipitation rates during the summer and maximum during the winter are observed. During March-April and September–November we find that the effect of precipitation on aerosols concentration is not clear owing to the indirect effects as compared with other studies over the Mediterranean basin where precipitation rate was shown as one of the strongest removal processes for atmospheric aerosols in winter [58]. As presented in Figure 3(a) the precipitation rate is very low ranging from 0.02 to 0.04 mm/month; hence, precipitation might have a lower contribution to the wet deposition of aerosols. The possible cause for the lower AOD values

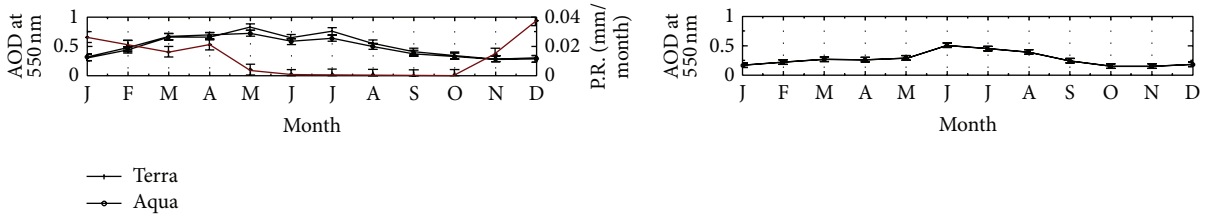

(a) Region 3 (b) Region 4

Figure 3: Climatology MODIS monthly AOD means over (a) region 3 (EP) from Terra and Aqua (2003–2013), the right axis is for the precipitation rate of the EP for the same period, (b) region 4 (Rub al Khali) with standard deviations.

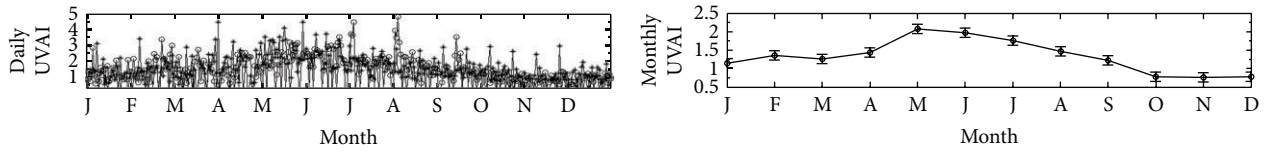

(a) (b)

Figure 4: (a) The monthly climatology means of UVAI over region 3 (EP) for 2012-2013 and (b) is Daily OMI UVAI for 2012-2013. The vertical bars represent standard errors.

can be precipitation over the source regions or precipitation during the aerosol travel from source to the observation site. If this is not the case, the most probable cause is the seasonal change of the wind stream pattern, which advects the aerosols from the source regions to the observation site as well as higher summer AODs due to accumulation of fine aerosol particles in summer [58]. It is noteworthy that annual dust and anthropogenic pollutants are the main emission sources during March-April and September–November periods. Despite the fact that the available precipitation data suffer from errors, they still can be used for long time averaging [59].

Terra mean AOD results were higher than Aqua during May–August; however the difference is not significantly high, consistent with [38] where they showed that there is no significant difference between Terra and Aqua results. The monthly climatology means over Rub al Khali Desert (Region 4) displays a maximum AOD_{550} value of 0.5035 ± 0.03 and a minimum of 0.1469 ± 0.03 representing lower monthly AOD as compared to that over region 3. This is attributed to the industrial activities and local air pollution over region 3.

3.2. Absorbing Aerosol Characteristics, Vertical Structure, and Subtypes. Absorbing aerosols, originating from arid areas, have long-range transport capability, during which they usually interact with urban/industrial pollutants and other aerosols under various meteorological conditions. Such transport results in a complex mixing scenario among different aerosols, affecting the climate system radiative balance directly and indirectly [2, 60]. To detect and quantify these aerosols, such as carbonaceous and mineral dust, the near-UV aerosol sensing is adequate since they absorb ultraviolet (UV) radiation.

The UVAI data used in this study are sensitive to dust vertical distribution, wind-transport, and the dust size distributions, which is a reasonable approach for arid environments [61]. Figures 4(a) and 4(b) present the daily OMI UVAI variations for 2012-2013 and monthly climatology means of the two-year period over region 3 (EP). We observe perennial positive values indicating the existence of absorbing aerosols all year round [62]. The daily UVAI observations highlight a monthly component during the 2-year period with a clear spike during late spring and summer seasons which is evident from the UVAI monthly climatology showing maxima of 2.1 ± 0.13 in May (Figure 4(b)). The high UVAI values during May are consistent with large AOD values observed from the MODIS data (Figure 3(a)) as compared to those observed over region 4. This leads us to believe in the presence of higher air pollution levels over region 3, representing the oil rich eastern province of Saudi Arabia. It is evident that MODIS AOD and UVAI show a similar pattern in aerosol variability (Figures 3 and 4) yet with sharper AOD peaks during summer. This is owed to the UVAI sensitivity to aerosol layer height [62], where the dust aerosols exist in a wider range of altitudes than possible anthropogenic aerosols, which are confined to the planetary boundary layer (PBL) [26, 28], where UVAI tends to be insensitive to these boundary layer aerosols [63]. This mixing scenario between aerosols of natural and anthropogenic origin is observed from the aerosols vertical backscatter and subtypes obtained from CALIPSO which is quite useful here for observing weak aerosol layers and thin clouds by detecting optical depths of 0.01 or less [64]. In Figure 5, the vertical profiles of the atmosphere up to 20 km, represented by total attenuated backscatter at 532 nm, are shown as CALIPSO overpasses the Eastern part of inland Saudi Arabia on 11 March (Figure 5(a))

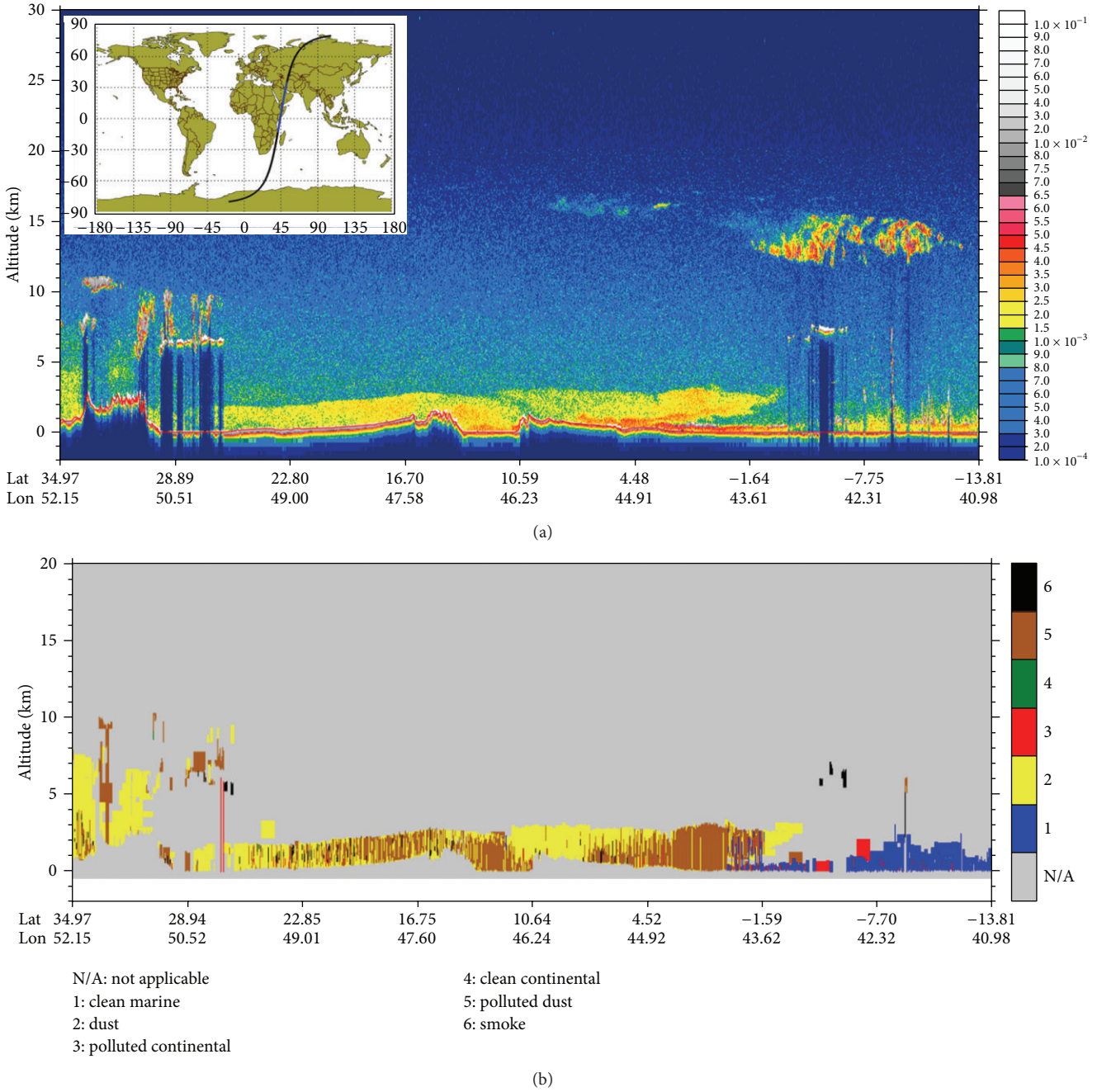

Figure 5: CALIPSO (a) total attenuated backscatter at 532 nm of a dust storm event as measured by the night-time CALIPSO overpass over the inland Saudi Arabia (at 2238 to 2251 UTC 11 March 2008) and (b) aerosol subtype over the same area. The surface elevation is shown as a thick black line. The inset map shows the path of CALIPSO overpass over the globe (black line) and the study region (red line).

during nighttime, while Figure 5(b) showed the most abundant aerosol types over selected areas shown in Figure 5(a). The profile clearly shows the vertical structure of a major SDS over the study regions. On 11 March, high concentration of aerosol reached high >5 km over the northern Eastern region and up to 2-3 km over the central and southern areas in the Eastern inland Saudi Arabia, including surrounding Gulf States. Areas in Eastern Africa are mostly covered by clouds, which show extremely high backscatter (topped white) and block backscatter from the atmosphere (Deep Blue) below them. Mixed cloud layers are observed over region of interest mainly dominated by dust and polluted dust starting at very high altitudes reflecting the fine mode fraction particles distribution which is mainly abundant over the northern part. The major SDS was also identified in other parameters obtained from CALIPSO, such as perpendicular attenuated backscatter (532 nm), total attenuated backscatter at 1064 nm, attenuated color ratio, and depolarization ratio (not shown).

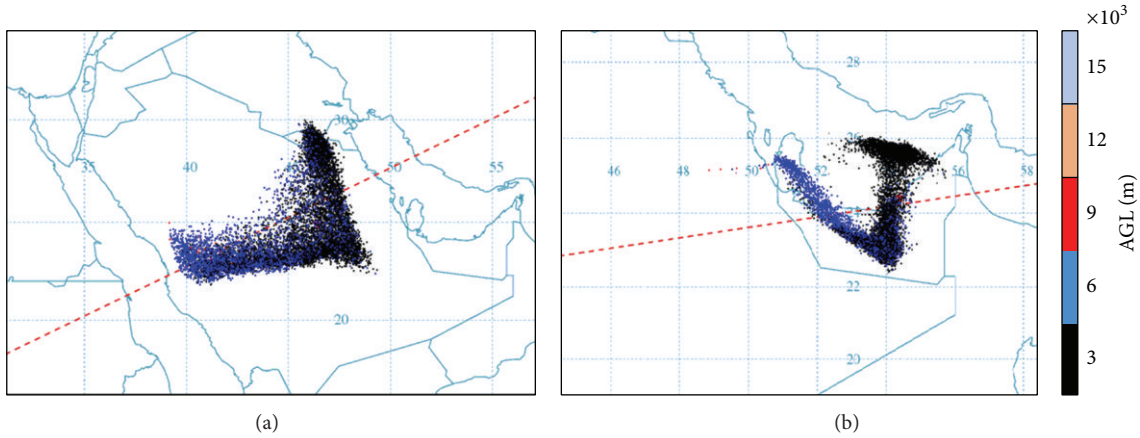

Figure 6: HYSPLIT backward trajectory dispersion starting from (a) Solar Village, (b) MASDAR ends on March 09, 2009 13:00 UTC. Heights are indicated by the legend bar.

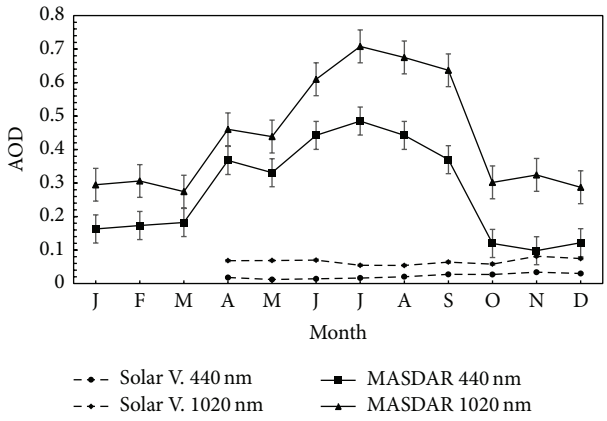

Figure 7: AERONET AOD observations at 440 and 1020 nm from April 2012 to May 2013 using Solar Village and MASDAR stations. The vertical bars represent standard errors.

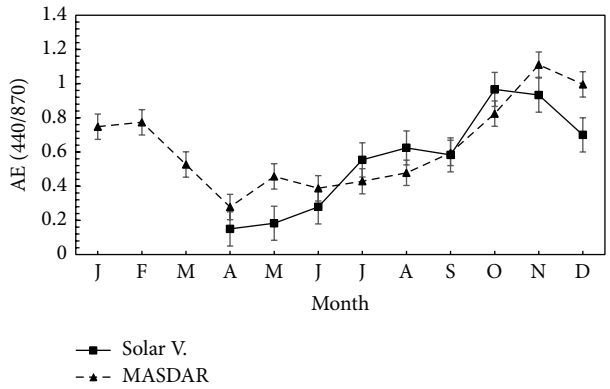

Figure 8: AERONET AE observations using MASDAR from April 2012 to May 2013 using MASDAR station. The vertical bars represent standard errors.

3.3. Microphysical Properties. AERONET ground-based measurements of AOD data at 440 nm and 1020 nm are analyzed for the available periods of April 2012–December 2012 for Solar Village and from June 2012 till May 2103 for MASDAR to verify satellite data as discussed in Sections 1 and 2.5. As previously discussed we considered the Solar Village location as an AOD representative over desert, while the MASDAR one to represent the AOD over the EP of Saudi Arabia. Moreover, the HYSPLIT backward trajectories shown in Figures 6(a) and 6(b) emphasize the fact that regions 3 and 4 are one of the possible sources of aerosols received at the Solar Village and MASDAR, respectively. The observations from both stations at 440 nm show maxima of 0.71 in July and a minimum of 0.27 in March over MASDAR and a maxima of 0.08 in November and a minimum of 0.05 in August over Solar Village (Figure 7). The high July AOD value (0.71) over MASADR showed a close agreement with the July AOD value (0.76) retrieved from Aqua over the EP, which confirms a general agreement between satellite and MASDAR AOD observations. However, such agreement was not established between the August AOD value (0.39) from Aqua over region 4 as compared to the AOD low value (0.05) recorded by the Solar Village station. This is expected owing to aerosols deposition taking place as they move from Rub al Khali to the Solar Village for a long distance (Figure 6(a)). It is clear that the AOD values at 440 nm are higher than those at 1020 nm since the longer wavelength is greatly affected by water-vapor absorption and hence is used to derive the total water-vapor column [24].

We use the AERONET AE (440/870) to identify the aerosol origin being natural, anthropogenic, or mixed over regions 3 and 4 of Saudi Arabia where small AE values are associated with large dust particles (natural origin) as compared to large AE values representing small size aerosols (anthropogenic/mixed) (Figure 8). The results show small AE values during spring (mostly desert dust) and larger AE values are observed during July–December mainly associated with smaller particles over MASDAR and Solar Village reflecting a more mixed scenario over both locations. This is attributed to the fact that pollutants as well as mixed aerosols with dust are quite common over Arabia. This is further

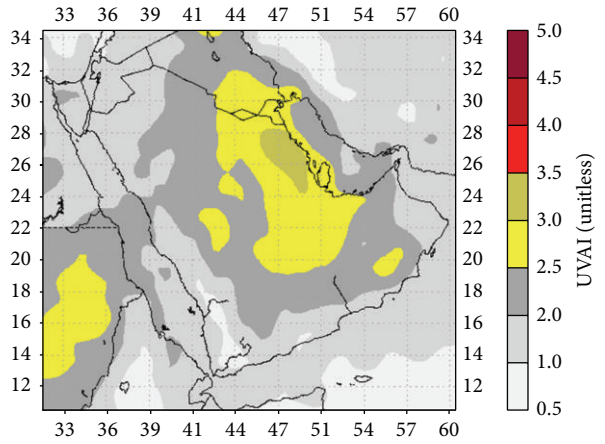

Figure 9: OMI UVAI image over Saudi Arabia on March 09, 2009.

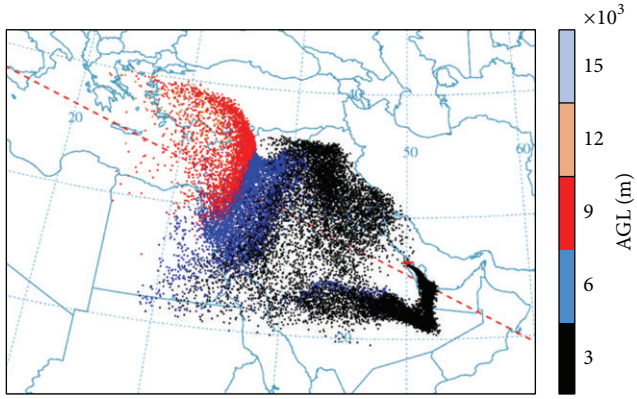

Figure 10: HYSPLIT backward trajectory dispersion starting from region 3 on March 09, 2009 16:00 UTC for 3 days. Heights are indicated by the legend bar.

observed from the OMI UVAI data over Saudi Arabia during March 9, 2009 dust storm event where the high UVAI values near region 3 indicate absorbing aerosols mixed with possibly desert dust, where the contribution of small particles from industrial emissions is attributed to the land-breeze circulations in this area [65] (Figure 9). Furthermore, particles' dispersion at different altitudes was observed at 16:00 UTC on March 09, 2009 by examining 3-day back trajectories originating from region 3. The trajectories computed by the HYSPLIT model initiated at 50 m above the ground level show that dust originated from the North West of Saudi Arabia and the east of Egypt where aerosols showed high dominancy at ~3000 m (Figure 10). However, the middle of the desert where Solar Village is located exhibits mixed particles at 3000 (black) and 6000 (blue) m showing higher deposition as aerosols approach the EP and agreeing with the small AERONET AE values around the springtime favoring dust presence (Figure 10).

MISR AOD, size, and shape fractions data was used to characterize the types of aerosol based on their physical and optical properties to study aerosols microphysics. The MISR AOD at 558 nm data categorizes particles into small, medium, and large sizes as well as to spherical and nonspherical. Figures 11(a) and 11(b) present the monthly size and shape averages, from 2003 to 2013 over region 3 where the large and small size particles' fraction showed higher dominancy than the medium ones (Figure 11(a)) with even more large size particles abundance during spring season. Such particle size occurrence agrees with the AE values with distinct dusty versus anthropogenic episodes as compared to mixed ones. It is also noticed that spherical particles are higher than nonspherical and show a more stable value all year round indicating high pollution levels. However, the nonspherical particles are significantly higher during March–July than the rest of the year (Figure 11(b)) which is consistent with the dust storms season extending from March till late summer [14]. The AOD of nonspherical particles reaches a maximum in June with a value of ~0.3517 ± 0.01, where the maximum of the spherical fraction AOD occurs in July with a value of ~0.4867 ± 0.01. The large AOD fractions are higher during March-May with a significant contribution from the desert dust, while during the rainy season, November–February, the AOD of small, medium and large particles significantly drops as expected.

Table 2: MISR AOD monthly mean size fractions for the period 2003–2013.

	MISR AOD average size fractions		
	Small	Medium	Large
January	0.0418	0.0418	0.1202
February	0.0418	0.0418	0.165
March	0.085	0.0983	0.2667
April	0.275	0.1583	0.3583
May	0.333	0.2733	0.385
June	0.3267	0.2233	0.33
July	0.3633	0.2033	0.3883
August	0.3367	0.075	0.3067
September	0.2233	0.05	0.18
October	0.1283	0.05	0.16
November	0.0633	0.05	0.0933
December	0.05	0.05	0.0783

During spring and summer seasons the MISR AOD generally shows higher values for large and small size particles as compared to the medium ones shown in Table 2. These high values during these seasons disclose that most particles are of large sizes with a radius larger than 1 μm especially for April and May. However, the October distribution shows that both small and large particles exists with more domination of large particles as can be revealed from the two peaks at ~0.1 and ~4 μm (Figure 12). The above results related to AOD, AE, and size distribution during spring and other seasons agrees with the spring maximum local desert-dust activity as well as mixed scenarios during other seasons [66].

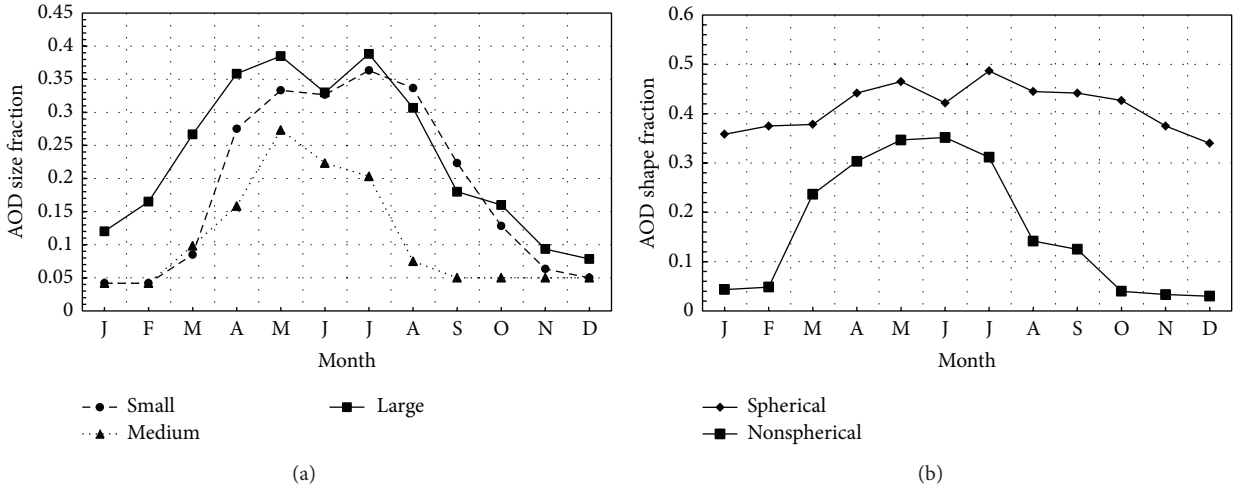

Figure 11: Climatology of AOD shape fraction and size over region 3 using MISR Level 3 at 558 nm (green band) (2003–2013): (a) size and (b) shape.

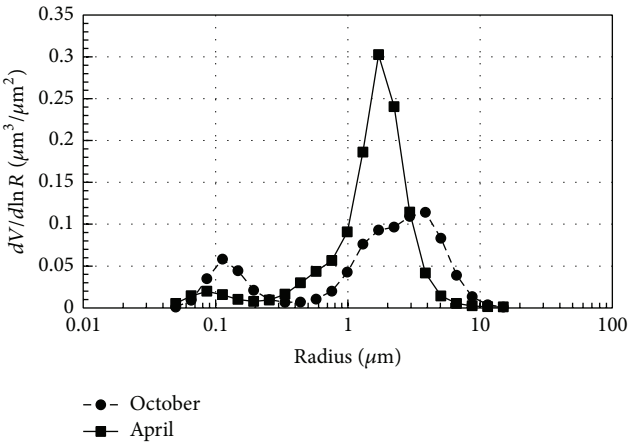

Figure 12: Size distribution of AERONET station at Solar Village in April 2012 and October 2012.

4. Conclusions

Sand-dust storms (SDSs) over the gulf region affect human life in various aspects including health and economy. They can be associated with climate change and result in different feedback mechanisms as well as with air pollution. Therefore, early detection and monitoring of SDSs is a matter of the utmost importance for possible risk reduction caused by these hazardous phenomena. Generally, satellite sensing using various sensors equipped for different purposes, provides synthetic ways of monitoring SDSs most effectively. In this study, multisensor approach is applied to severe SDS cases, which originated in Arabia and from the surroundings, to investigate characteristics of the case storm and to explore the capability of such approaches for its detection and monitoring. For this purpose, we employ several satellite sensors, namely, MODIS, OMI, and the lidar instrument and visible-infrared imagers on-board CALIPSO and data from the AERONET ground stations. Information on aerosol loading is provided by AOD retrieved from the Terra/Aqua MODIS. For retrieving AOD over bright land surface, DB algorithm was adopted. For the dust storm event, information on dust clouds was obtained by the standard AOD except over the bright surface areas around Rub al Khali (Empty Quarter) Desert, which were covered by DB AOD. This indicates that combined aerosol loading information available from other algorithms (and sensors) provide more continuous and complete detection of severe SDSs.

Overall the multisensor approach using satellite remote sensing provides useful information on various properties of the dust storm event, including location and magnitude of aerosol loading, size mode of aerosols, the behavior of long-lived absorbing aerosols, and the vertical structure. This enables us to make more continuous and complete detection of severe SDSs. In addition, our approach provides information on anthropogenic aerosols and pollutants, not just dust particles. Early detection of such aerosols and pollutants is especially very useful and important for health protection in the areas located downstream from the source region.

Conflict of Interests

The authors declare that there is no conflict of interests regarding the publication of this paper.

Acknowledgments

The authors would like to acknowledge the support provided by King Abdulaziz City for Science and Technology (KACST) for funding this work under Grant no. MT-32-76. The support provided by the Deanship of Research at King Fahd University of Petroleum & Minerals (KFUPM) is gratefully acknowledged. Analyses and visualizations used in this study were produced with the Giovanni online data

system, developed and maintained by the NASA GES DISC. They also acknowledge the MODIS mission scientists and associated NASA personnel for the production of the data used in this research effort. Furthermore, the authors would like also to acknowledge the use of the Samueli Laboratory in Computational Sciences in the Schmid College of Science and Technology, Chapman University, for image processing and data analysis.

References

[1] M. D. King, Y. J. Kaufman, D. Tanré, and T. Nakajima, "Remote Sensing of Tropospheric Aerosols from Space: Past, Present, and Future," *Bulletin of the American Meteorological Society*, vol. 80, no. 11, pp. 2229–2259, 1999.

[2] Y. J. Kaufman, D. Tanré, and O. Boucher, "A satellite view of aerosols in the climate system," *Nature*, vol. 419, no. 6903, pp. 215–223, 2002.

[3] K. K. Moorthy, V. S. Nair, S. S. Babu, and S. K. Satheesh, "Spatial and vertical heterogeneities in aerosol properties over oceanic regions around india: implications for radiative forcing," *Quarterly Journal of the Royal Meteorological Society*, vol. 135, no. 645, pp. 2131–2145, 2009.

[4] P. Ginoux, D. Garbuzov, and N. C. Hsu, "Identification of anthropogenic and natural dust sources using moderate resolution imaging spectroradiometer (MODIS) deep blue level 2 data," *Journal of Geophysical Research D: Atmospheres*, vol. 115, no. 5, 2010.

[5] T. M. Saeed, H. Al-Dashti, and C. Spyrou, "Aerosol's optical and physical characteristics and direct radiative forcing during a shamal dust storm: a case study," *Atmospheric Chemistry and Physics*, vol. 14, no. 7, pp. 3751–3769, 2014.

[6] J. Heinrich and R. Slama, "Fine particles, a major threat to children," *International Journal of Hygiene and Environmental Health*, vol. 210, no. 5, pp. 617–622, 2007.

[7] Y. Aboel Fetouh, H. El Askary, M. El Raey, M. Allali, W. A. Sprigg, and M. Kafatos, "Annual patterns of atmospheric pollutions and episodes over Cairo Egypt," *Advances in Meteorology*, vol. 2013, Article ID 984853, 11 pages, 2013.

[8] W. A. Sprigg, S. Nickovic, J. N. Galgiani et al., "Regional dust storm modeling for health services: the case of valley fever," *Aeolian Research*, vol. 14, pp. 53–73, 2014.

[9] H. El-Askary, R. Gautam, R. P. Singh, and M. Kafatos, "Dust storms detection over the Indo-Gangetic basin using multi sensor data," *Advances in Space Research*, vol. 37, no. 4, pp. 728–733, 2006.

[10] A. I. Rushdi, K. F. Al-Mutlaq, B. R. T. Simoneit et al., "Characteristics of lipid tracer compounds transported to the Arabian Gulf by runoff from rivers and atmospheric dust transport," *Arabian Journal of Geosciences*, vol. 3, no. 2, pp. 113–131, 2010.

[11] A. I. Rushdi, K. F. Al-Mutlaq, M. Al-Otaibi, A. H. El-Mubarak, and B. R. T. Simoneit, "Air quality and elemental enrichment factors of aerosol particulate matter in Riyadh City, Saudi Arabia," *Arabian Journal of Geosciences*, vol. 6, no. 2, pp. 585–599, 2013.

[12] J. M. Prospero, P. Ginoux, O. Torres, S. E. Nicholson, and T. E. Gill, "Environmental characterization of global sources of atmospheric soil dust identified with the Nimbus 7 Total Ozone Mapping Spectrometer (TOMS) absorbing aerosol product," *Reviews of Geophysics*, vol. 40, no. 1, pp. 2-1–2-31, 2002.

[13] P. P. Pease, V. P. Tchakerian, and N. W. Tindale, "Aerosols over the Arabian Sea: geochemistry and source areas for aeolian desert dust," *Journal of Arid Environments*, vol. 39, no. 3, pp. 477–496, 1998.

[14] B. H. Alharbi, A. Maghrabi, and N. Tapper, "The march 2009 dust event in Saudi Arabia: precursor and supportive environment," *Bulletin of the American Meteorological Society*, vol. 94, no. 4, pp. 515–528, 2013.

[15] M. Notaro, F. Alkolibi, E. Fadda, and F. Bakhrjy, "Trajectory analysis of Saudi Arabian dust storms," *Journal of Geophysical Research D: Atmospheres*, vol. 118, no. 12, pp. 6028–6043, 2013.

[16] A. Maghrabi, B. Alharbi, and N. Tapper, "Impact of the March 2009 dust event in Saudi Arabia on aerosol optical properties, meteorological parameters, sky temperature and emissivity," *Atmospheric Environment*, vol. 45, no. 13, pp. 2164–2173, 2011.

[17] T. A. Jones and S. A. Christopher, "Seasonal variation in satellite-derived effects of aerosols on clouds in the Arabian Sea," *Journal of Geophysical Research D: Atmospheres*, vol. 113, no. 9, Article ID D09207, 2008.

[18] I. Sabbah and F. M. Hasan, "Remote sensing of aerosols over the Solar Village, Saudi Arabia," *Atmospheric Research*, vol. 90, no. 2-4, pp. 170–179, 2008.

[19] A. Smirnov, B. N. Holben, O. Dubovik et al., "Atmospheric aerosol optical properties in the Persian Gulf," *Journal of the Atmospheric Sciences*, vol. 59, no. 3, pp. 620–634, 2002.

[20] H. Kutiel and H. Furman, "Dust storms in the Middle East: sources of Origin and their temporal characteristics," *Indoor and Built Environment*, vol. 12, no. 6, pp. 419–426, 2003.

[21] J. Barkan, H. Kutiel, and P. Alpert, "Climatology of dust sources in North Africa and the Arabian Peninsula, based on TOMS data," *Indoor and Built Environment*, vol. 13, no. 6, pp. 407–419, 2004.

[22] H. M. El-Askary, S. Sarkar, M. Kafatos, and T. A. El-Ghazawi, "A multisensor approach to dust storm monitoring over the nile delta," *IEEE Transactions on Geoscience and Remote Sensing*, vol. 41, no. 10, pp. 2386–2391, 2003.

[23] H. El-Askary and M. Kafatos, "Dust storm and black cloud influence on aerosol optical properties over Cairo and the greater Delta Region, Egypt," *International Journal of Remote Sensing*, vol. 29, no. 24, pp. 7199–7211, 2008.

[24] H. El-Askary, R. Farouk, C. Ichoku, and M. Kafatos, "Intercontinental transport of dust and pollution aerosols across Alexandria, Egypt," *Annales Geophysicae*, vol. 27, no. 7, pp. 2869–2879, 2009.

[25] S. A. Christopher and T. A. Jones, "Satellite and surface-based remote sensing of Saharan dust aerosols," *Remote Sensing of Environment*, vol. 114, no. 5, pp. 1002–1007, 2010.

[26] H. S. Marey, J. C. Gille, H. M. El-Askary, E. A. Shalaby, and M. E. El-Raey, "Study of the formation of the 'black cloud' and its dynamics over Cairo, Egypt, using MODIS and MISR sensors," *Journal of Geophysical Research D: Atmospheres*, vol. 115, no. 21, Article ID D21206, 2010.

[27] A. K. Prasad, H. El-Askary, and M. Kafatos, "Implications of high altitude desert dust transport from Western Sahara to Nile Delta during biomass burning season," *Environmental Pollution*, vol. 158, no. 11, pp. 3385–3391, 2010.

[28] H. S. Marey, J. C. Gille, H. M. El-Askary, E. A. Shalaby, and M. E. El-Raey, "Aerosol climatology over Nile Delta based on MODIS, MISR and OMI satellite data," *Atmospheric Chemistry and Physics*, vol. 11, no. 20, pp. 10637–10648, 2011.

[29] T. M. Saeed and H. Al-Dashti, "Optical and physical characterization of 'Iraqi freedom' dust storm, a case study," *Theoretical and Applied Climatology*, vol. 104, no. 1-2, pp. 123–137, 2011.

[30] R. R. Draxler, D. A. Gillette, J. S. Kirkpatrick, and J. Heller, "Estimating PM10 air concentrations from dust storms in Iraq, Kuwait and Saudi Arabia," *Atmospheric Environment*, vol. 35, no. 25, pp. 4315–4330, 2001.

[31] S. M. Mohalfi, H. S. Bedi, T. N. Krishnamurti, and S. D. Cocke, "Impact of shortwave radiative effects of dust aerosols on the summer season heat low over Saudi Arabia," *Monthly Weather Review*, vol. 126, no. 12, pp. 3153–3168, 1998.

[32] A. S. Ahmed, A. A. Adel, and A. A. Mohammed, "Airborne dust size analysis for tropospheric propagation of millimetric waves into dust storms," *IEEE Transactions on Geoscience and Remote Sensing*, vol. GE-25, no. 5, pp. 593–599, 1987.

[33] H. A. Al-Jeelani, "Air quality assessment at Al-Taneem area in the Holy Makkah City, Saudi Arabia," *Environmental Monitoring and Assessment*, vol. 156, no. 1–4, pp. 211–222, 2009.

[34] H. A. Al-Jeelani, "The impact of traffic emission on air quality in an urban environment," *Journal of Environmental Protection*, vol. 4, no. 2, pp. 205–217, 2013.

[35] A. I. Rushdi, A. H. El-Mubarak, L. Lijotra et al., "Characteristics of organic compounds in aerosol particulate matter from Dhahran city, Saudi Arabia," *Arabian Journal of Chemistry*, 2014.

[36] B. N. Holben, T. F. Eck, I. Slutsker et al., "AERONET—a federated instrument network and data archive for aerosol characterization," *Remote Sensing of Environment*, vol. 66, no. 1, pp. 1–16, 1998.

[37] R. R. Draxler, B. Stunder, G. Rolph, A. Stein, and A. Taylor, *HYSPLIT4 User's Guide Version 4.9*, 2009, http://www.arl.noaa.gov/documents/reports/hysplit_user_guide.pdf.

[38] L. A. Remer, Y. J. Kaufman, D. Tanré et al., "The MODIS aerosol algorithm, products, and validation," *Journal of the Atmospheric Sciences*, vol. 62, no. 4, pp. 947–973, 2005.

[39] R. C. Levy, L. A. Remer, R. G. Kleidman et al., "Global evaluation of the Collection 5 MODIS dark-target aerosol products over land," *Atmospheric Chemistry and Physics*, vol. 10, no. 21, pp. 10399–10420, 2010.

[40] Y. J. Kaufman, D. Tanré, L. A. Remer, E. F. Vermote, A. Chu, and B. N. Holben, "Operational remote sensing of tropospheric aerosol over land from EOS moderate resolution imaging spectroradiometer," *Journal of Geophysical Research D: Atmospheres*, vol. 102, no. 14, pp. 17051–17067, 1997.

[41] Y. J. Kaufman, A. E. Wald, L. A. Remer, B.-C. Gao, R.-R. Li, and L. Flynn, "MODIS 2.1-μm channel-correlation with visible reflectance for use in remote sensing of aerosol," *IEEE Transactions on Geoscience and Remote Sensing*, vol. 35, no. 5, pp. 1286–1298, 1997.

[42] N. C. Hsu, S.-C. Tsay, M. D. King, and J. R. Herman, "Aerosol properties over bright-reflecting source regions," *IEEE Transactions on Geoscience and Remote Sensing*, vol. 42, no. 3, pp. 557–569, 2004.

[43] N. C. Hsu, S. C. Tsay, M. D. King, and J. R. Herman, "Deep blue retrievals of Asian aerosol properties during ACE-Asia," *IEEE Transactions on Geoscience and Remote Sensing*, vol. 44, no. 11, pp. 3180–3195, 2006.

[44] R. C. Levy, S. Mattoo, L. A. Munchak et al., "The Collection 6 MODIS aerosol products over land and ocean," *Atmospheric Measurement Techniques*, vol. 6, no. 11, pp. 2989–3034, 2013.

[45] J. V. Martonchik, D. J. Diner, K. A. Crean, and M. A. Bull, "Regional aerosol retrieval results from MISR," *IEEE Transactions on Geoscience and Remote Sensing*, vol. 40, no. 7, pp. 1520–1531, 2002.

[46] J. V. Martonchik, D. J. Diner, R. A. Kahn, B. J. Gaitley, and B. N. Holben, "Comparison of MISR and AERONET aerosol optical depths over desert sites," *Geophysical Research Letters*, vol. 31, no. 16, 2004.

[47] J. V. Martonchik, R. A. Kahn, and D. J. Diner, "Retrieval of aerosol properties over land using MISR observations," in *Satellite Aerosol Remote Sensing Over Land*, A. Kokhanovsky, Ed., pp. 267–293, Springer, Berlin, Germany, 2009.

[48] R. A. Kahn, B. J. Gaitley, M. J. Garay et al., "Multiangle Imaging SpectroRadiometer global aerosol product assessment by comparison with the Aerosol Robotic Network," *Journal of Geophysical Research D: Atmospheres*, vol. 115, no. 23, Article ID D23209, 2010.

[49] R. A. Kahn, B. J. Gaitley, J. Martonchik, D. Diner, K. Crean, and B. N. Holben, "MISR global aerosol optical depth validation based on two years of coincident AERONET observations," *Journal of Geophysical Research—Atmospheres*, vol. 110, Article ID D10S04, 2005.

[50] D. M. Winker, J. Pelon, and M. P. McCormick, "The CALIPSO mission: spaceborne lidar for observation of aerosols and clouds," in *3rd Lidar Remote Sensing for Industry and Environment Monitoring*, vol. 4893 of *Proceedings of SPIE*, pp. 1–11, Hangzhou, China, March 2003.

[51] P. F. Levelt, G. H. J. van den Oord, M. R. Dobber et al., "The ozone monitoring instrument," *IEEE Transactions on Geoscience and Remote Sensing*, vol. 44, no. 5, pp. 1093–1100, 2006.

[52] O. Torres, P. K. Bhartia, A. Sinyuk, E. J. Welton, and B. N. Holben, "Total Ozone Mapping Spectrometer measurements of aerosol absorption from space: comparison to SAFARI 2000 ground-based observations," *Journal of Geophysical Research D: Atmospheres*, vol. 110, no. 10, Article ID D10S18, pp. 1–12, 2005.

[53] O. Torres, A. Tanskanen, B. Veihelmann et al., "Aerosols and surface UV products form Ozone Monitoring Instrument observations: an overview," *Journal of Geophysical Research D: Atmospheres*, vol. 112, no. 24, Article ID D24S47, 2007.

[54] B. N. Holben, D. Tanré, A. Smirnov et al., "An emerging ground-based aerosol climatology: aerosol optical depth from AERONET," *Journal of Geophysical Research D: Atmospheres*, vol. 106, no. 11, pp. 12067–12097, 2001.

[55] O. Dubovik, A. Smirnov, B. N. Holben et al., "Accuracy assessments of aerosol optical properties retrieved from Aerosol Robotic Network (AERONET) sun and sky radiance measurements," *Journal of Geophysical Research D: Atmospheres*, vol. 105, no. 8, pp. 9791–9806, 2000.

[56] S. Dey and L. Di Girolamo, "A climatology of aerosol optical and microphysical properties over the Indian subcontinent from 9 years (2000–2008) of Multiangle Imaging Spectroradiometer (MISR) data," *Journal of Geophysical Research D: Atmospheres*, vol. 115, no. 15, Article ID D15204, 2010.

[57] H. El-Askary and M. Kafatos, "Dust storm and black cloud influence on aerosol optical properties over Cairo and the Greater Delta region, Egypt," *International Journal of Remote Sensing*, vol. 29, no. 24, pp. 7199–7211, 2008.

[58] C. D. Papadimas, N. Hatzianastassiou, N. Mihalopoulos, X. Querol, and I. Vardavas, "Spatial and temporal variability in

aerosol properties over the Mediterranean basin based on 6-year (2000–2006) MODIS data," *Journal of Geophysical Research D: Atmospheres*, vol. 113, no. 11, Article ID D11205, 2008.

[59] R. Kistler, E. Kalnay, W. Collins et al., "The NCEP-NCAR 50-year reanalysis: Monthly means CD-ROM and documentation," *Bulletin of the American Meteorological Society*, vol. 82, no. 2, pp. 247–267, 2001.

[60] C. Ahn, O. Torres, and P. K. Bhartia, "Comparison of ozone monitoring instrument UV aerosol products with aqua/moderate resolution imaging spectroradiometer and multiangle imaging spectroradiometer observations in 2006," *Journal of Geophysical Research D: Atmospheres*, vol. 113, no. 16, Article ID D16S27, 2008.

[61] K. Schepanski, I. Tegen, B. Laurent, B. Heinold, and A. Macke, "A new Saharan dust source activation frequency map derived from MSG-SEVIRI IR-channels," *Geophysical Research Letters*, vol. 34, no. 18, Article ID L18803, 2007.

[62] O. Torres, P. K. Bhartia, J. R. Herman, Z. Ahmad, and J. Gleason, "Derivation of aerosol properties from satellite measurements of backscattered ultraviolet radiation: theoretical basis," *Journal of Geophysical Research D: Atmospheres*, vol. 103, no. 14, pp. 17099–17110, 1998.

[63] N. M. Mahowald and J.-L. Dufresne, "Sensitivity of TOMS aerosol index to boundary layer height: implications for detection of mineral aerosol sources," *Geophysical Research Letters*, vol. 31, no. 3, Article ID L03103, 2004.

[64] M. J. McGill, M. A. Vaughan, C. R. Trepte et al., "Airborne validation of spatial properties measured by the CALIPSO lidar," *Journal of Geophysical Research D: Atmospheres*, vol. 112, no. 20, Article ID D20201, 2007.

[65] T. F. Eck, B. N. Holben, J. S. Reid et al., "Spatial and temporal variability of column-integrated aerosol optical properties in the southern Arabian Gulf and United Arab Emirates in summer," *Journal of Geophysical Research D: Atmospheres*, vol. 113, no. 1, 2008.

[66] A. Smirnov, B. N. Holben, O. Dubovik et al., "Atmospheric aerosol optical properties in the Persian Gulf," *Journal of the Atmospheric Sciences*, vol. 59, no. 3, pp. 620–634, 2002.